IEEE Access
Multidisciplinary | Rapid Review | Open Access Journal

Received 29 May 2024, accepted 17 June 2024, date of publication 24 June 2024, date of current version 1 July 2024.

Digital Object Identifier 10.1109/ACCESS.2024.3418434

RESEARCH ARTICLE

Dynamic A-MPDU Adaptation Method for Airtime Fairness in Channel Bonding-Ready WLANs

HITOMI TAMURA[1], (Member, IEEE), DAIKI NOBAYASHI[2], (Member, IEEE), KENJI KAWAHARA[3], (Member, IEEE), AND KAZUYA TSUKAMOTO[3], (Member, IEEE)

[1]Faculty of Engineering, Fukuoka Institute of Technology, Fukuoka 811-0295, Japan
[2]Faculty of Engineering, Kyushu Institute of Technology, Kitakyushu, Fukuoka 804-8550, Japan
[3]Department of Computer Science and Networks, Kyushu Institute of Technology, Iizuka, Fukuoka 820-8502, Japan

Corresponding author: Hitomi Tamura (h-tamura@fit.ac.jp)

This work was supported in part by Japan Society for the Promotion of Science under KAKENHI under Grant 23K11092; and in part by the Commissioned Research by the National Institute of Information and Communications Technology (NICT), Japan, under Grant JPJ012368C05501.

ABSTRACT Channel bonding is a technology that increases the transmission rates by bundling and using multiple continuous channels. However, its communication performance decreases over time because of the channel competition caused by nearby wireless LAN devices. Dynamic channel bonding (DCB) is projected to become mainstream based on efficient channel utilization, which can overcome this performance degradation even under severe competitive conditions. However, because the implementation of the DCB in actual hardware products and simulators is still in the preliminary stage, its performance has not been evaluated in detail. The performance of DCB has not been evaluated at the frame level with carrier-sense multiple access/collision avoidance (CSMA/CA) functions under diverse channel competition conditions. In this study, we employed a theoretical approach ($2\times$M/M/1/K) based on the frame level to evaluate the performance of DCB with the CSMA/CA function. Furthermore, we implemented a channel bonding mechanism in the Scenargie simulator and verified its effectiveness by comparing the simulation results with theoretical results. The simulation results show that the DCB inevitably undergoes performance degradation owing to a performance anomaly caused by airtime unfairness. Therefore, we propose a dynamic A-MPDU adaptation method to achieve airtime fairness among the nearby wireless LANs. The proposed method can maximize throughput performance while achieving airtime fairness.

INDEX TERMS Airtime fairness, A-MPDU, dynamic channel bonding, Wi-Fi.

I. INTRODUCTION

With the rapid development of mobile devices and expansion of various applications, the monthly global average usage per smartphone is projected to exceed 20 GB by the end of 2023 [1]. IEEE 802.11ax (hereinafter "11ax") is a wireless standard for coping with such rapid increases in traffic and high-density Wi-Fi environments. Furthermore, 11ax improves the throughput of the WLAN by up to 9.6 Gb/s [2]. 11ax devices were commercialized in late 2020. The 11ax features include orthogonal frequency division multiple access (OFDMA), 1,024 QAM, channel bonding (CB), multiuser multiple-input multiple-output (MU-MIMO), and BSS-coloring. CB and MU-MIMO use multiple channels/antennas for high-speed communications. Furthermore, IEEE 802.11be, which enables further high-throughput performance through multilink operations by aggregating multiple radio interfaces of one pair of access points (APs) and stations (STAs), is currently considered an emerging Wi-Fi standard for standardization. Wi-Fi technology enables high-throughput performance by bundling physical interfaces, channels, or antennas.

Herein, we focus on CB technology, one of the 11ax's technologies [3]. The CB achieves high-throughput communication by bundling and simultaneously using multiple continuous channels. However, in an actual dense WLAN environment, channel competition between multiple Wi-Fi devices is inevitable because of the deep penetration of

The associate editor coordinating the review of this manuscript and approving it for publication was Hosam El-Ocla.

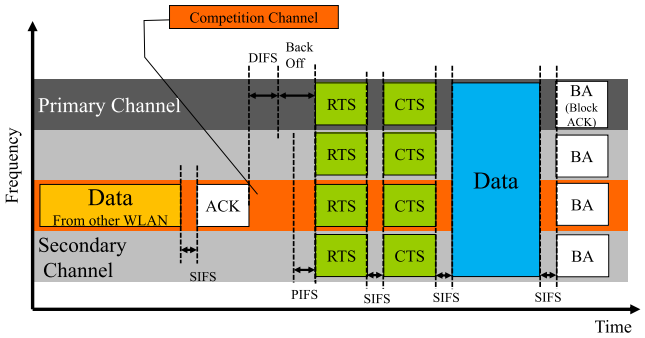

FIGURE 1. Static channel bonding (SCB) with channel competition from nearby WLAN (80-MHz SCB).

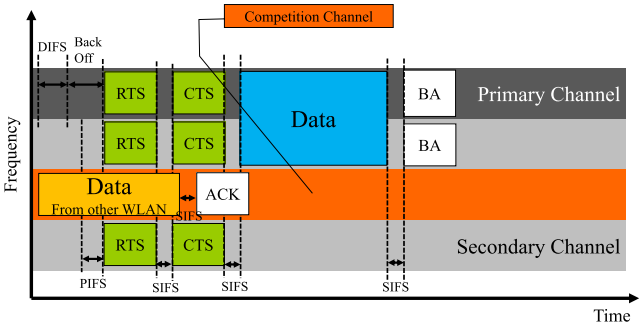

FIGURE 2. Dynamic channel bonding (DCB) with channel competition from nearby WLAN (80-MHz DCB).

Wi-Fi networks. Because channel competition can cause significant performance degradation, two bonding channel management methods- static CB (SCB) and dynamic CB (DCB) [4]- are employed to mitigate their negative impacts on communication performance. When some channels to be bonded are occupied for other communications (channel competition), the SCB must wait until the end of the channel competition, and the predetermined number of bonded channels is always used for communication, as shown in Fig. 1. Alternatively, the DCB shrinks the channel width until there is no channel overlap and then maintains communication without interruption, as shown in Fig. 2. Therefore, the DCB can improve the efficiency of channel utilization compared to that of the SCB, even when the channel is contended by multiple communications. In this case, the width of the bonded channel changes dynamically at every transmission time of each frame, and its transmission rate changes frequently.

Furthermore, because the aggregation of MAC protocol data unit (aggregated-MPDU, A-MPDU) was mandatory in IEEE 802.11n (hereinafter "11n"), IEEE 802.11ac (hereinafter "11ac") and 11ax, the overhead of stop-and-wait automatic repeat request (ARQ) can be decreased. In 11n/ac/ax, aggregation MAC service data unit (A-MSDU) can also be used but it is optional. The A-MPDU aggregates multiple MPDUs comprising a MAC header, payload, and frame check sequence (FCS). It aggregates multiple payloads with only a MAC header and FCS. When a frame error is detected, all aggregated payloads must be retransmitted in the case of the A-MSDU, whereas, only the error frame is retransmitted in the case of the A-MPDU.

When the size of the A-MPDU is fixed, the communication duration required for each frame transmission (hereinafter "airtime") is considerably different, particularly in the case of the DCB. The difference in airtime among frames severely affects the communication performance of all wireless devices, which is referred to as "performance anomaly (PA)" [5]. Because DCB has not been well implemented in real WLAN devices and simulators, their performance has been extensively investigated. In this study, we evaluated DCB performance based on the frame level through theoretical analysis and simulations. First, we evaluated the DCB performance analytically by applying the queueing theory [7]. We then modified the Scenargie simulator [6] to apply the DCB, and verified the performance of the developed DCB. Furthermore, we compare the simulation results of the developed DCB with our analytical results. Based on the obtained results, we propose a dynamic A-MPDU adaptation method to overcome the PA problem caused by the DCB function and implement the proposed method in the Scenargie simulator [7]. Through simulations, we evaluated the performance of the developed method in a channel competition environment.

The major contributions of this paper are summarized as follows:

- We promote the implementation of the DCB function in Scenargie, which has not yet been implemented in actual WLAN APs.
- We analytically evaluated the effectiveness of the DCB using queueing theory and verified the reliability of the DCB function implemented in Scenargie by comparing its results with the analytical results.
- We propose a dynamic A-MPDU adaptation method to overcome the PA problem in the DCB.
- We demonstrate the effectiveness of the proposed method through simulations.

The rest of this paper is organized as follows: Section II explains the basics of the CB and FA; Section III reviews some related reports; Section IV describes the queueing analysis of 40-MHz DCB with a channel competition environment; Section V describes the proposed dynamic A-MPDU size adaptation method; Section VI presents the simulation results; Section VII discusses the limitations of our proposed method and our future research; and Section VIII summarizes the study.

II. CHANNEL BONDING AND FRAME AGGREGATION IN IEEE 802.11 WLAN

IEEE 802.11n/ac/ax includes both the CB and FA as high-speed communication technologies for WLAN.

FA enables the simultaneous transmission of frames and can improve the performance of wireless networks by reducing the overhead of CSMA/CA associated with

transmitting small packets. This reduces the 802.11 protocol overhead because multiple packets can be sent with a single set of PHY and MAC headers instead of each packet having its own headers. The numbers of ACKs and interframe spaces were also reduced. Two FA methods were defined: A-MPDU and A-MSDU.

The A-MSDU (Fig. 3) aggregates MSDUs, which are frames with an MSDU subframe header received by the MAC from the upper layer. Two or more subframes are bundled together and placed in an 802.11 MAC frame, and a MAC header and trailer are added. The A-MSDUs are transmitted using a single PHY header.

The A-MPDU (Fig. 4) aggregates MPDUs, one of which has a MAC header and a trailer. Multiple MPDUs were bundled and transmitted using a PHY header. The A-MPDU aggregates the MPDUs; therefore, only the MPDUs with errors can be retransmitted. However, if an A-MSDU is applied, the entire A-MSDU frame should be retransmitted even if some MSDUs have errors.

CB is a promising technology with broad bandwidth that uses multiple adjacent channels. A CB enables high-speed communication; however, it can be used only when multiple adjacent channels are not busy. Therefore, two CB types are defined: static CB (SCB) and dynamic CB (DCB). Suppose an AP with SCB; the AP will wait to send data frames until all channel sets for SCB are clear. Meanwhile, an AP with a DCB will use only clear and adjacent channels, including the primary channel; in other words, only some channels set for the DCB will be used when it is applied.

In CB, the communication band comprises of one primary channel (20 MHz) and one or more secondary channels. Suppose an AP operates with SCB, where the AP communicates only when all channels preliminarily set in the AP are simultaneously clear. The request-to-send (RTS)/clear-to-send (CTS) function is applied for channel access (Fig. 1), where channel(s) is the measured duration of the PIFS in the secondary channel(s). If a CTS is generated as a response to the RTS in the entire channel, the sender node can send its data frame to its destination. If other WLAN communications are detected, the sender must wait until all channels are clear.

Comparatively, suppose an AP operates with a DCB in which the AP communicates with available continuous channels from the primary channel and the RTS/CTS function is applied for channel access (Fig. 2). If a CTS is generated as a response to the RTS in some channels, the sender node can send its data frame to its destination within continuous, clear channels. If another WLAN communication is detected, the sender uses only clear 1,2, or 4 channel(s) in the DCB.

In SCB, preliminary set channels were used for data transmission. Therefore, the bandwidth is fixed and stable; however, transmission rights are difficult to obtain simultaneously if other WLANs on the secondary channel(s) frequently transmit data, and the waiting time until all channels are clear can be lengthened. The DCB uses only the continuous clear channels from the primary channel. Thus, it can efficiently use the channels. However, the bandwidth is easily variable and unstable if other WLANs in the secondary channel(s) frequently use the channel. Suppose that frames of the same size are transmitted using DCB. The airtime of data transmission differs significantly depending on whether the channel width is reduced.

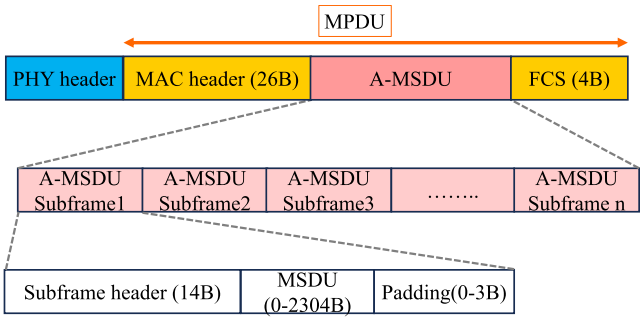

FIGURE 3. A-MSDU frame format.

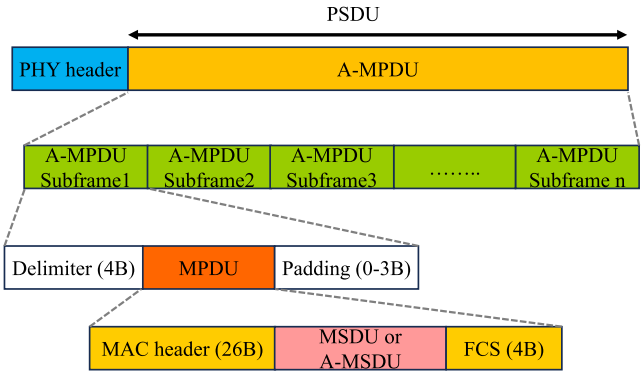

FIGURE 4. A-MPDU frame format.

Therefore, to increase the throughput performance and airtime fairness if the channel width is unstable, we propose adaptively aggregating the frames in an A-MPDU frame based on the channel width of the WLAN using DCB.

III. RELATED WORKS

Previous studies have investigated the effects of FA on WLAN. These studies mainly focused on improving the throughput using A-MPDU, A-MSDU, or a combination of both, depending on the bit error rate (BER) of the channel and Wi-Fi environment (SNR, node movement, and density) [8], [9], [10], [11]. The authors in [12] and [13] analytically investigated the impact of the BER and payload size on the effectiveness of A-MPDU and A-MSDU in IEEE 802.11n. They improved the throughput at the MAC layer by choosing either A-MPDU or A-MSDU frame aggregation in IEEE 802.11n without considering dynamic changes in the aggregated frame size. In [14], the authors analytically improved the performance of A-MPDU frame aggregation compared with that of A-MSDU and proposed a dynamic method for adjusting the number of aggregated frames of A-MPDU depending on the BER of the channel. In [15], frame aggregation was used to improve the energy efficiency

of IEEE 802.11n/ac WLANs. A dynamic A-MPDU frame sizing scheme considering the energy consumption in a WLAN using a channel with a high error rate was proposed to improve the throughput performance and energy efficiency through experiments in a Linux-based lab-level testbed. Reference [16] proposed an adaptive selection method for the number of aggregated frames and rate selection, depending on the BER. These studies aimed to change the number of aggregated frames based on the BER of a channel but did not consider PA. Reference [17] treated airtime fairness in sharing a wireless channel between two heterogeneous stations, known as the PA problem, with different data rates and frame sizes. The authors proposed a frame-size adaptation scheme that controls the number of aggregated frames, data rate, and selection of A-MPDU and A-MSDU to overcome the PA problem in IEEE 802.11n WLAN.

Reference [18] proposed a method that estimates the average delay of MPDUs for each queue of enhanced distributed channel access (EDCA) and clarified the optimal number of aggregated MPDUs for each queue to maximize the system throughput while satisfying the delay requirement of each queue in IEEE 802.11ac. Reference [19] also considered the delay requirement of the VoIP application.

In addition, [20] proposed a queueing-based solution for the PA problem in cases where the AP connects to some STAs with heterogeneous Wi-Fi standards, and investigated the airtime distribution of user datagram protocol (UDP) downlink traffic using a Linux-based system. The authors employed multiple traffic identifier queues and proposed the enqueue and dequeue methods to achieve airtime fairness. However, these studies did not consider channel bonding or competition in WLAN. In this study, we achieved airtime fairness between two competing WLANs using another channel bandwidth.

References [21] and [22] discussed the effects on throughput and fairness of CB types and how to use the secondary channels in DCB in WLANs by using a Markov chain. Furthermore, [23] revealed the adaptive environment of DCB and SCB, and the appropriate bandwidth depending on the CB type and Wi-Fi environment using Markov chains.

For airtime adaptation, [24] proposed the transmission opportunity (TXOP) duration adaptation for FA on IEEE 802.11ac and discussed its performance depending on the method of EDCA Access Categories (ACs) employed. This study calculated the maximum TXOP duration and number of aggregated frames that were adapted within the TXOP limit. Similarly, [25] applied FA and size adaption to minimize the power consumption period and achieve energy efficiency in IEEE 802.11ad.

Previous studies have discussed the appropriate FA method, frame size, CB type, and CB bandwidth for various Wi-Fi environments; however, they did not consider the differences in the airtime and frame size adaptation of A-MPDU between shrunken and unshurunk widths in WLAN with DCB.

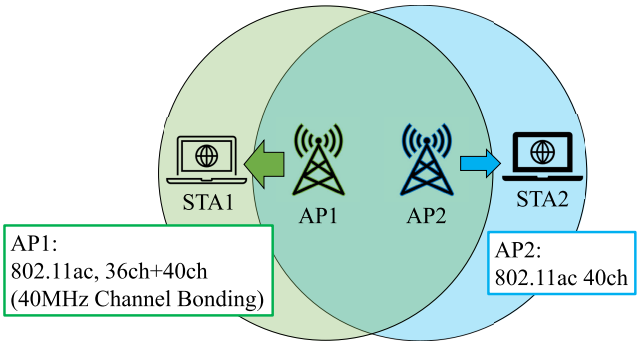

FIGURE 5. Network model.

IV. PERFORMANCE ANALYSIS OF DCB USING THE QUEUEING THEORY

Bianchi's performance evaluation method [26] is a typical analytical method for evaluating the performance of conflict models in WLAN channel. Bianchi's model expresses the back-off counter and stage of each terminal in a Markov chain, and evaluates the performance of a WLAN operating in a distributed coordination function (DCF) when multiple terminals compete in a channel. Performance evaluation at frame level can be achieved using a queueing system. However, it can only consider the conflict model in a channel in a WLAN, and cannot model an AP simultaneously using multiple channels. However, performance evaluation considering CSMA/CA and CB through experiments [27], simulations [28], and analytical approaches [29], [30] have been reported. However, none of these studies simultaneously considered CSMA/CA, DCB behavior in the presence of multiple WLANs, or performance evaluation at the frame level. Therefore, we define the number of frames in a buffer waiting for transmission as the status of the 11ac AP interface. Then, we consider the transmission time of one frame, including the DCF interframe space (DIFS), average back-off time, short interframe space (SIFS), and sending ACK frame, as the frame transmission time. Thus, we can analytically evaluate the performance of the DCB at the frame level using the queueing theory.

A. NETWORK MODEL

Fig. 5 shows the proposed network model. Two 11ac AP-STA pairs are deployed, and AP1-STA1 operates a 40-MHz-width DCB in 36 and 40 ch as its primary and secondary channels, respectively. Another AP-STA (AP2-STA2) does not operate the CB, and uses only 40 ch as its primary channel. Frames are transmitted from the APx to STAx ($x = 1, 2$). Specifically, AP2 usually transmits frames to STA2 in 40 ch of the 20-MHz bandwidth when AP2 obtains a transmission opportunity. On the other hand, AP1 transmits frames to STA1 with a CB of 40-MHz bandwidth when AP1 obtains transmission opportunity in 40 ch. Otherwise, AP1 transmits frames to STA1 in a single channel (only 36 ch) with a 20-MHz bandwidth. Channel competition occurs only

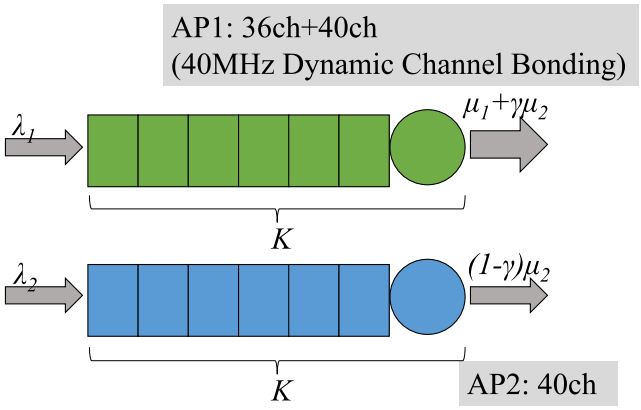

FIGURE 6. Queueing model of our network model.

in 40 ch based on the DCF. For example, channel competition occurs when AP1 transmits frames to STA1 and AP2 already obtains channel access and transmits frames to STA2. AP1 dynamically changes the bonding channel width based on the DCB algorithm.

B. APPLYING THE QUEUEING THEORY TO OUR NETWORK MODEL

In the evaluation model, we assume that the frame arrives at APx ($x = 1, 2$) with buffer size K according to a Poisson process with parameter λ_x, and the frame transmission rate follows a Poisson process with parameter μ_x. Therefore, the frame transmission from APx to STAx can be modeled by an M/M/1/K queueing system. In the proposed evaluation model, frame transmission is modeled in both 36 and 40 ch for two pairs of AP-STA; thus, the 2×M/M/1/K queueing system [31], which treats the statuses of two independent queueing systems simultaneously, is applied.

Fig. 6 shows the 2×M/M/1/K queueing system used in this study. When AP2 obtains a transmission opportunity in 40 ch, AP1 transmits a frame with μ_1 for 20-MHz bandwidth. On the other hand, when AP1 obtains a transmission opportunity in 40 ch, AP1 transmits a frame with $\mu_1+\mu_2$ for 40-MHz channel bonding. Here, parameter γ ($0 \le \gamma \le 1$) represents the average ratio of transmission opportunities with the CB of AP1. γ is defined as the probability of obtaining the channel access rights of AP1 on the secondary channel. Hence, γ depends on whether there are waiting frames in the buffer of AP2 buffer on the secondary channel, and is defined as follows:

- When the number of waiting frames in the buffer of AP2 is zero, because there is no waiting frame on AP2, AP1 can always use the secondary channel, 40 ch, to transmit frames with 40-MHz-bandwidth CB. Thus, the service rate of AP1 is always equal to $\mu_1 + \mu_2$; then, we could recognize that γ temporarily equals 1.
- When the number of waiting frames in the buffer of AP2 is not zero, because one or more waiting frames exist in AP2, the transmission opportunities of 40 ch by AP1 and AP2 compete in the CSMA/CA. If AP1 obtains a transmission opportunity of 40 ch with a predetermined probability γ, bonding across the 40-MHz bandwidth can be performed. Thus, the service rate was $\mu_1 + \mu_2$. However, if AP1 does not receive a transmission opportunity of 40 ch with probability $(1 - \gamma)$, AP1 transmits a frame using the 20-MHz-bandwidth. Thus, the service rate of AP1 is μ_1.

As described above, because the service rate of AP1 dynamically changes in response to the access determined by the CSMA/CA function in 40 ch, the frame transmission rate of AP1 is either μ_1 (20-MHz bandwidth) or $\mu_1+\mu_2$ (40-MHz bandwidth). However, the service rate changed according to the average bonding ratio γ. Therefore, the service rate of AP1 approximates $\mu_1 + \gamma\mu_2$, and that of AP2 approximates $(1 - \gamma\mu_2)$ from a long-term perspective. Thus, we applied the 2×M/M/1/K queueing system to the proposed evaluation model, as shown in Fig. 6.

Using a random variable $X^{(x)}(t)$, which represents the number of waiting frames in APx at a certain time t, we define the steady-state probability $p_i^{(x)}$ of APx as $p_i^{(x)} = \lim_{t\to\infty} \Pr\{X^{(x)}(t) = i; 0 \le i \le K\}$.

Then, we can obtain a balanced equation for AP1 as

$$\begin{aligned} \lambda_1 p_0^{(1)} &= (\mu_1 + \gamma\mu_2) p_1^{(1)}, \\ (\lambda_1 + \mu_1 + \gamma\mu_2)\, p_i^{(1)} &= \lambda_1 p_{i-1}^{(1)} + (\mu_1 + \gamma\mu_2) p_{i+1}^{(1)}, \\ &\quad \text{if } 0 < i < K, \\ \lambda_1 p_{K-1}^{(1)} &= (\mu_1 + \gamma\mu_2) p_K^{(1)}. \end{aligned} \tag{1}$$

Furthermore, we can also obtain a balanced equation for AP2 as follows:

$$\begin{aligned} \lambda_2 p_0^{(2)} &= (1 - \gamma)\mu_2 p_1^{(2)}, \\ (\lambda_2 + (1 - \gamma)\mu_2)\, p_i^{(2)} &= \lambda_2 p_{i-1}^{(2)} + (1 - \gamma)\mu_2 p_{i+1}^{(2)}, \\ &\quad \text{if } 0 < i < K, \\ \lambda_2 p_{K-1}^{(2)} &= (1 - \gamma)\mu_2 p_K^{(2)}. \end{aligned} \tag{2}$$

In the 2× M/M/1/K queueing system, we treat the two statuses of the two M/M/1/K queues simultaneously. Thus, we define the state transition matrix of APx as $\mathbf{Q}_x = [q_{l,m}^{(x)} = \lim_{\Delta t\to 0} \Pr\{X^{(x)}(t + \Delta t) = m | X^{(x)}(t) = l\}; 0 \le l \le K, 0 \le m \le K]$, the state transition matrix of each M/M/1/K queueing system can be derived from (1) and (2). Furthermore, 2× M/M/1/K queueing system can be constructed using two state transition matrices of each M/M/1/K queueing system as follows:

$$\mathbf{Q} = \mathbf{Q_1} \oplus \mathbf{Q_2}. \tag{3}$$

Here, we define a random variable vector $\boldsymbol{Z}(t)$, which indicates the entire system, as follows:

$$\mathbf{Z}(\mathbf{t}) = \left(X^{(1)}(t), X^{(2)}(t)\right). \tag{4}$$

Let $\mathbf{s_j} = \{(s_1, s_2); 0 \le s_i \le K, i = 1, 2\}(0 \le j < (K+1)^2)$ denote the state vector, which indicates the possible state space of the number of waiting frames in AP1 and

AP2, respectively. Subsequently, the steady-state probability $y_{\mathbf{s}_j}(= y_{(s_1,s_2)})$ is defined as follows:

$$y_{\mathbf{s_j}} = \lim_{t\to\infty} Pr\{\mathbf{Z(t)} = (s_1, s_2); 0 \le j < (K+1)^2\} \quad (5)$$

Furthermore, if $\mathbf{y} = [y_{\mathbf{s}_0}, y_{\mathbf{s}_1}, \cdots, y_{\mathbf{s}_k}, \cdots, y_{\mathbf{s}_{(K+1)^2-1}}]$ denote the steady state probability vector, then $\boldsymbol{y}$ and the state transition matrix $\mathbf{Q}$ satisfy the following equations:

$$\mathbf{yQ} = \mathbf{0}, \qquad \mathbf{ye} = 1, \quad (6)$$

where $\mathbf{0}$ is a raw vector with all elements equal to 0 for $\dim(\mathbf{0}) = (K+1)^2$, and $\mathbf{e}$ is a column vector with all elements equal to 1 for $\dim(\mathbf{e}) = (K+1)^2$. Therefore, the steady-state probability of the 2×M/M/1/K queueing system can be obtained by solving (6).

As described above, the simplest model with only one AP-STA pair in each of the 36 and 40 channels was assumed in the analytical model for the simplest explanation. In the model, if the number of AP and STA pairs and the traffic load can change, the superposition of multiple Poisson distributions is equal to the sum of the arrival rate, λ; hence, the number of AP-STA pairs can be increased by changing the λ value in the equations. Furthermore, γ is the probability of obtaining the transmission rights of 40 channels, γ enables the network model evaluation when SCB is applied to AP1. The SCB will only communicate with the channels if the AP receives a channel access right of the secondary channel to be bonded with probability γ (Fig. 6). Therefore, the performance of SCB can be evaluated by changing $(\mu_1 + \gamma\mu_2)$ in (1) to $\gamma(\mu_1 + \mu_2)$.

C. DEVIATION OF PERFORMANCE MEASURES

We used the bonding probability P_b and average throughput TH_1 of AP1 to evaluate the performance. AP1 can perform bonding when either the number of the waiting frames of AP2 is zero or AP1 obtains a transmission opportunity of 40 ch with probability γ by CSMA/CA. Therefore, the bonding probability P_b of AP1 can be expressed as:

$$P_b = \sum_{s_1=0}^{K} y_{(s_1,0)} + \gamma\left(1 - \sum_{s_1=0}^{K} y_{(s_1,0)}\right). \quad (7)$$

The average throughput TH_1 of AP1 is expressed as the sum of the achievable throughput of the CB and the throughput of only one channel as follows:

$$TH_1 = (\mu_1 + \mu_2)P_b + \mu_1(1 - P_b). \quad (8)$$

Furthermore, the average throughput TH_2 of AP2 is expressed as the throughput only when the secondary channel is available:

$$TH_2 = \mu_2(1 - P_b). \quad (9)$$

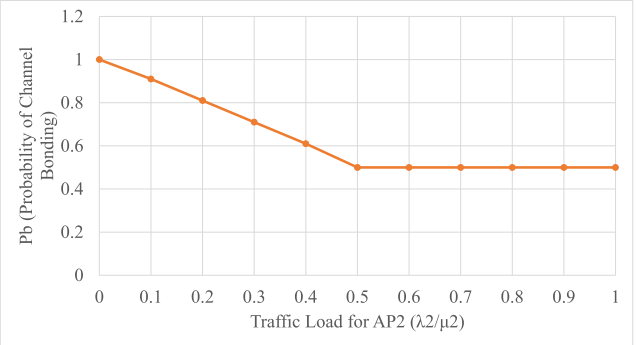

FIGURE 7. Probabilities of channel bonding (AP1).

D. PARAMETER SETTINGS

In this analysis, the service rate μ_x of APx was set as follows:

$$\mu_x = \frac{1}{\frac{framesize[bit]}{PHYrate[b/s]} + T\,[s]}, \quad (10)$$

$$T\,[s] = DIFS + slottime + \frac{CW_{min}}{2} + SIFS + ACK, \quad (11)$$

where PHY rate is the physical-level rate of the 11ac standards, and T is the average duration of DIFS, back-off time, SIFS, and ACK. We assume that both AP1 and AP2 use 11ac and frame aggregation functions; thus, the PHY rate of AP1 is 135 Mb/s when frames are transmitted by 40-MHz DCB, with a modulation scheme of 64 QAM and a coding rate of 5/6. In addition, when AP2 does not use CB, other settings remain the same as those of AP1, but the PHY rate becomes 65 Mb/s. Equations (8), (10), and (11) show the relationship between AP2 and DCB use.

E. ANALYTICAL RESULTS

First, we show the analytical results of a case in which AP1 uses 40-MHz DCB (e.g., 36 and 40 ch) and AP2 uses a 20-MHz secondary channel (40 ch). Therefore, AP2 did not employ channel bonding. We assumed that the A-MPDU size of AP2 is the same as that of AP1. In this analysis, the maximum number of waiting frames in the queue K, is set to 40. Furthermore, the service rate of AP1, μ_1, was set according to (10), and the frame service rate of AP1, λ_1, was set to $1.5\mu_1$. Thus, the traffic load is heavy for AP1. Furthermore, γ is set to 0.5 which means that there are two contended WLANs on the secondary channel, and they can obtain the channel access rights equally.

Fig. 7 shows the bonding probability P_b of AP1 derived from (7). The x-axis indicates the traffic load of AP2, that is, the channel utilization of the secondary channel of AP1. P_b linearly decreased as the traffic load of AP2 increased; however, it remains at 0.5 when the traffic load of AP2 was greater than 0.5 because the transmission opportunities for AP1 and AP2 were equal.

Figs. 8 and 9 show the impact of A-MPDU size on the average throughput of AP1 and AP2, respectively. The x-axis indicates the traffic load of AP2, and the y-axis indicates

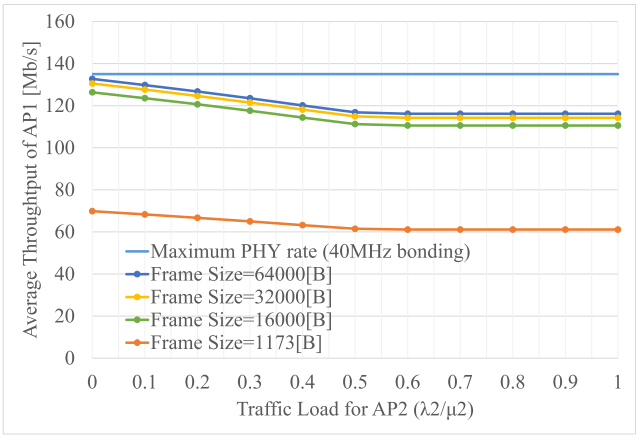

FIGURE 8. Impact of A-MPDU size on the average throughput of AP1.

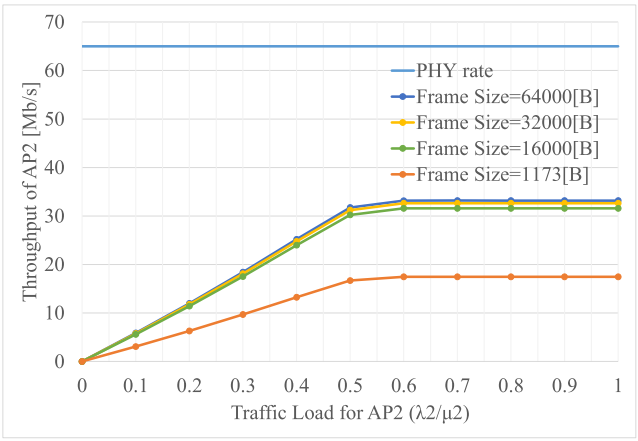

FIGURE 9. Impact of A-MPDU size on the average throughput of AP2.

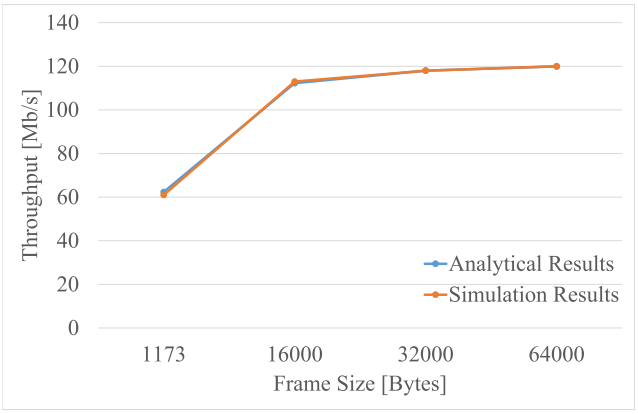

FIGURE 10. Throughput of AP1 when $\rho_2 = 0$.

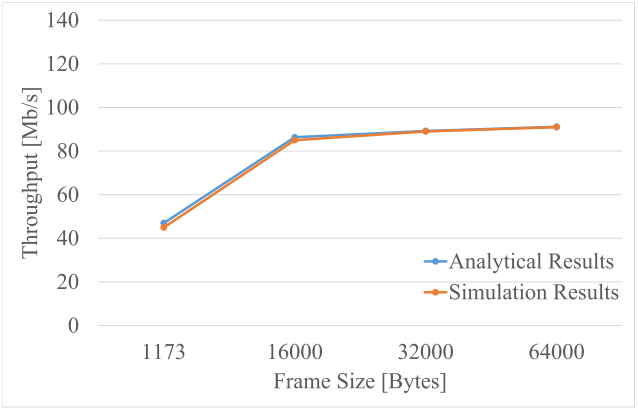

FIGURE 11. Throughput of AP1 when $\rho_2 = 1$.

the average throughput. The average throughput of AP1 decreases as the traffic load of AP2 increases (Fig. 8). However, the average throughput of AP2 increases as the traffic load of AP2 increases. Furthermore, the average throughput of AP1 and AP2 increases as the frame size (A-MPDU size) increases. In the case where the frame size is 1,173 bytes, the overhead of the CSMA/CA expressed in (11) is large. Thus, the average throughput of AP1 and AP2 is lower than that of when the frame size was larger. When the frame size increases, AP1 and AP2 can transmit more bits per transmission opportunity. Therefore, the A-MPDU should be large. However, the frame sizes of AP1 and AP2 were equal, and the airtime of AP2 was twice that of AP1. Furthermore, if the frame size was 64,000 bytes, the throughput of AP1 was stable at a maximum PHY rate of 0.8, whereas that of AP2 was stable at a PHY rate of 0.5. Thus, an imbalance in the throughput of both APs affects both the wireless LANs.

Therefore, we should equalize the airtime of APs competing in a channel. However, we could not dynamically change A-MPDU size during the analysis. Therefore, we modified the simulator and used it to evaluate the proposed A-MPDU-size adaptation method.

F. VALIDITY VERIFICATION OF THE MODIFIED SIMULATOR

We implemented the DCB algorithm in Scenargie 2.2 and compare the communication performance of the simulator and the analytical model described in this section. For example, the throughput of AP1 obtained using Scenargie is compared to the analytical results obtained from (8), (10), and (11). Furthermore, we implemented the DCB algorithm in Scenargie 2.2 as described in Section II.

In the simulation, we assume that AP1 uses DCB but AP2 does not, and the parameters in Section IV-D are applied. However, the traffic model differed from the analysis, and a constant bit rate (CBR) with UDP was assumed in the simulation. The traffic generation rate of AP1, λ_1, was set to $1.5\mu_1$, and μ_1 depended on the frame size. In both the analysis and simulation, we assumed that the traffic load was heavy; therefore, the differences in the packet generation models had no significant impact on the performance evaluation. Furthermore, in the analytical model, we assumed that the frame size includes transport, IP, and MAC headers (MPDU delimiter, MAC header, and FCS); however, the simulation results did not include these headers. Suppose that one frame includes a 1,500 Byte payload, which includes a UDP header (8 bytes), an IP header (20

bytes), application data, and MAC headers (34 bytes, which is the sum of the MPDU delimiter, MAC header, and FCS). The header overhead was 1, 472/1, 534. Thus, in this section, the throughput values obtained by the analysis are multiplied by 1, 472/1, 534 for comparison with the simulation results.

Figs 10 and 11 show the throughput of the simulation and theoretical analysis, respectively. Both results vary with the change in frame size, where the utilization of AP2, ρ_2, is 0 or 1. The throughput obtained from the simulations was almost the same as that calculated by the analysis for both cases of $\rho_2 = 0$ and 1. Therefore, the modified DCB simulator was effective for the performance evaluation.

V. PROPOSED METHOD: DYNAMIC A-MPDU SIZE ADAPTATION METHOD

A. IN THE CASE OF FIXED A-MPDU SIZE

The airtime for each frame transmission in the 11ac WLAN can significantly differ from each other because the PHY rate fluctuates owing to the DCB function (i.e., shrinking of the channel width), and the A-MPDU size is predetermined and fixed by each AP. Diverse airtime inherently cause PA [3], resulting in performance degradation. To overcome the PA problem and maintain fairness with contended communication, there is a need to adjust the airtime (duration of frame transmission), considering the effect of shrinking the channel width in the DCB. For example, if a small A-MPDU is employed at the AP with a DCB, because the number of frame transmission opportunities for a certain period is increased, the number of channel assessments for CB and the probability of CB increase, but the number of bits transmitted by one frame remains small. By contrast, if a large A-MPDU is employed at the AP with DCB, the number of channel assessments for CB and the probability of CB decrease owing to the decrease in the number of frame transmissions in a certain period. However, the number of bits transmitted by a single frame increases. This indicates a trade-off between the probability of frame transmission by CB and the amount of data transmitted by one A-MPDU frame, as shown in Fig. 12. Consequently, the goal of our proposal is to adapt the airtime, namely, the A-MPDU size of the DCB, based on the number of frame transmission opportunities and the available bandwidth fluctuated by the DCB of each frame for airtime fairness between competitive WLANs.

B. DYNAMIC A-MPDU SIZE ADAPTATION METHOD

To achieve the goal described in Subsection V-A, we propose an A-MPDU-size adaptation method in which the size of the A-MPDU dynamically changes in response to the width of the available channels determined by the DCB mechanism. The proposed scheme allows the best utilization of channel resources for efficient communication in the secondary channel. We assume that two contended WLANs, one of which uses the DCB function and the other does not use the CB, and attempt to obtain a channel right at the secondary channel. The outline of the proposed scheme is as follows.

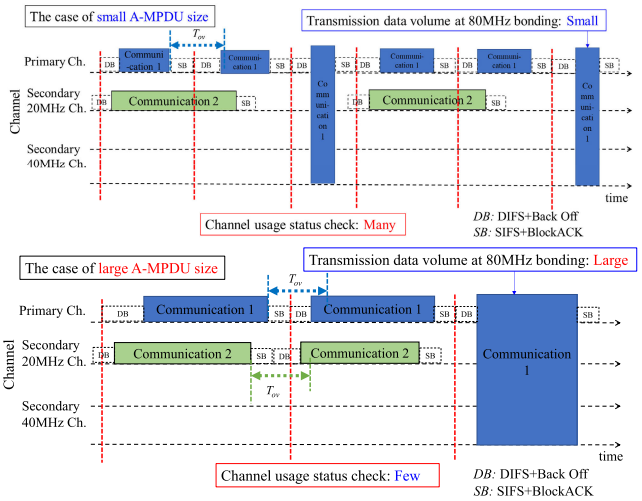

FIGURE 12. Trade-off between the probability of frame transmission by CB and the amount of transmitted data by one A-MPDU frame.

We assume that the number of contended WLANs in the secondary channel is set to n, and we assume $n = 2$ for a simple explanation of our proposed method. In the secondary channel, there are two contended communications, one of which is Communication 1 (C-1) and the other is Communication 2 (C-2). We then define the following requirements for C-1 and C-2.

- Thr requirement for C-2: $\frac{1}{n}$ for the maximum throughput should be guaranteed, where n is the number of contended communications on the same channel. In this case, 50% ($\frac{1}{n}$) throughput should be guaranteed.
- Requirement for C-1: Throughput performance should be maximized while satisfying C-2's requirement.

To satisfy the requirement for C-2, we equalize the sum of airtime for C-1 and C-2 on the secondary channel. Simultaneously, we increased the airtime for C-1 on the bonded channels (80 MHz) as much as possible, thereby improving the throughput performance of C-1. To achieve this, we adjust not only the number of frame transmissions but also their airtime on the bonded channels (whose width is expressed here as X MHz). Because these parameters highly depend on the shrinkage of the channel width (whose width is here after expressed as Y MHz), the airtime (AT) determined by both the A-MPDU size and the PHY rate significantly affects the communication performance. Parameters X and Y MHz in the DCB are defined as follows:

- DB: Duration of DIFS + Back-off
- AT_{CBR1-X} (AT_{CBR1-Y}): Transmission duration of one frame when C-1 transmits at X (or Y) MHz width.
- AT_{CBR2}: Transmission duration of one frame on C-2.

AT includes all durations (DB, data transmission, and ACK). Herein, we consider only a case where AT_{CBR1-Y} is greater than AT_{CBR2}. AT_{CBR1-X} which satisfies the requirements for C-1 and C-2 simultaneously are calculated using the following equations: Notably, AT_{CBR1-Y} is an input parameter for calculating AT_{CBR1-X}. If we define the duration

of C-2 on the secondary channel as $TIME_{C2}$, the following equation can be derived to satisfy the requirement for C-2:

$$AT_{CBR1-X} = TIME_{C2}, \\ = AT_{CBR2} \cdot x. \quad (12)$$

where x is the number of frame transmissions in $TIME_{C2}$. In this case, x depends on the lengths of AT_{CBR1-Y} and AT_{CBR2} and can be expressed as follows:

$$x = \frac{AT_{CBR1-Y}}{AT_{CBR2}}. \quad (13)$$

The expected number of frame transmissions for C-2 in $TIME_{C2}$ is expressed as E_x. The probability of frame transmissions for C-1 owing to CSMA/CA is approximately $1/n$. In such a case, if C-2 achieves frame transmission two consecutive times (the probability is $\frac{1}{n^2}$), C-2 can occupy the secondary channel for 2×airtime of x. Thus, the available airtime increases with the number of consecutive acquisitions of transmission opportunities, k. In summary, the expected airtime E_{AT_x} can be expressed as:

$$E_{AT_x} = E_x \cdot AT_{CBR2}, \\ = AT_{CBR2} \cdot x \cdot \sum_{k=1}^{\infty} k \left(\frac{1}{n}\right)^k. \quad (14)$$

Because (14) is the sum of an arithmetic-geometric sequence with a common difference k and a common ratio $1/n$, E_{AT_x} can be expressed as:

$$E_{AT_x} = AT_{CBR2} \cdot x \cdot n. \quad (15)$$

From (12), (13), and (15), AT_{CBR1-X} can be expressed as

$$AT_{CBR1-X} = n \cdot AT_{CBR1-Y}. \quad (16)$$

If the bonded channel is shrunk to Y MHz, CSMA/CA and ACK transmissions occur n times for n frame transmissions on average during AT_{CBR1-X} in the secondary channel. Therefore, the overhead of CSMA/CA and ACK transmission should be reduced, and the optimal AT_{CBR1-X} value is given by

$$AT_{CBR1-X} = n \cdot AT_{CBR1-Y} - (n-1) \cdot T_{ov}, \quad (17)$$

where T_{ov} indicates the overhead of one frame transmission, which is defined as the sum of DB, airtime of the PHY header, SIFS, and airtime of the ACK frame.

Finally, if the message segment size of the original packet is MSS bit and the PHY rate of X MHz width is R_X Mb/s, the appropriate A-MPDU frame size PKT_X MHz can be expressed as follows:

$$PKT_{CBR1-X} = AT_{CBR1-X} \cdot \frac{R_X}{MSS}. \quad (18)$$

In the proposed method, the optimal number of aggregate frames can be calculated using (17) and (18) to determine whether the channel width of the bonding AP is shrunken or bonded. In the equations, the airtime of one frame (that is, the non-aggregated frame) transmission of the competing AP is required, and we assume that it can be obtained by measuring the busy period of the secondary channel in the bonding AP. Therefore, information exchange between the APs is not needed and the bonding AP can autonomously calculate the optimal number of aggregate frames depending on its bonding width.

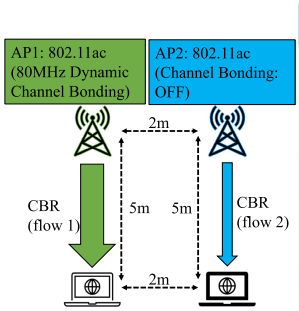

Setting Items	Settings
Channels to use (flow 1)	100, 104, 108, 112ch (Primary Channel: 100ch)
Channel to use (flow 2)	108 ch
Maximum A-MPDU size	flow1:64[pkt], flow2:1[pkt]
Modulation method	20MHz : 256QAM 3/4 40MHz : 256QAM 5/6 80MHz : 256QAM 5/6
Payload size	1472 [Byte]
Transmission rate	flow 1 = 433.3[Mb/s] (80MHz) flow 1 = 200.0[Mb/s] (40MHz) flow 2 = 86.7[Mb/s] (20MHz)
Guard Interval	Short Guard Interval

FIGURE 13. Simulation environment.

VI. PERFORMANCE EVALUATION

In this study, we evaluated the DCB performance when the width of the bonded channels was dynamically changed to either 80 or 40 MHz. Notably, this competition pattern is likely to occur in actual environments. Therefore, we set $X = 80$ and $Y = 40$ in (18); hereafter, this situation is referred to as 80–40-MHz DCB. Note that we evaluated the DCB performance in other competitive environments, but we show only the results for $X = 80$ and $Y = 40$ herein for brevity.

A. SIMULATION ENVIRONMENT

In this study, we verified the effectiveness of the A-MPDU-size adaptation method described in the previous section using Scenargie 2.2, in which the DCB was implemented. Fig. 13 shows the simulation environment and settings. Two pairs of AP and STA were deployed. The distance between the AP and STA was 5 m, and the distance between each pair was 2 m. Each AP sent a CBR flow to each STA with the transmission rate shown in Fig. 13. DCB communication (hereinafter "flow 1") occurs from AP1 to STA1 and communication from AP2 to STA2 competes with flow 1 (hereinafter "flow 2"). flow 1 performs DCB up to 80-MHz bandwidth in the environment, as shown in Fig. 14. During the simulation, flows 1 and 2 were generated by the CBR/UDP from 4 to 16 s, and the seed value was randomly changed 10 times.

To verify the effectiveness of (18), we compared the 80–40-MHz DCB using (18) with a method that employed a fixed A-MPDU frame size (conventional method as 11ac). In the proposed method, we effectively used communication in a wide channel by adjusting the A-MPDU size dynamically according to the available channel width. To satisfy the

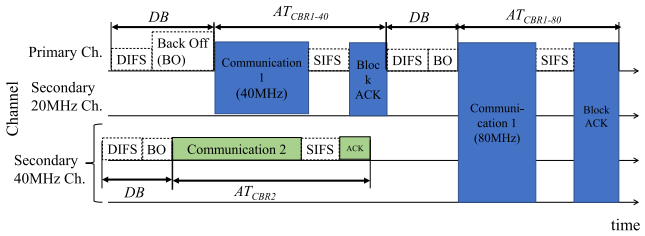

FIGURE 14. Definition of parameter values in 80–40-MHz DCB.

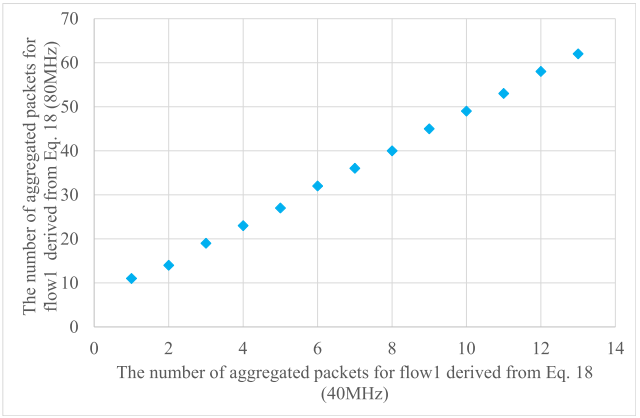

FIGURE 15. Number of aggregated packets derived from (18).

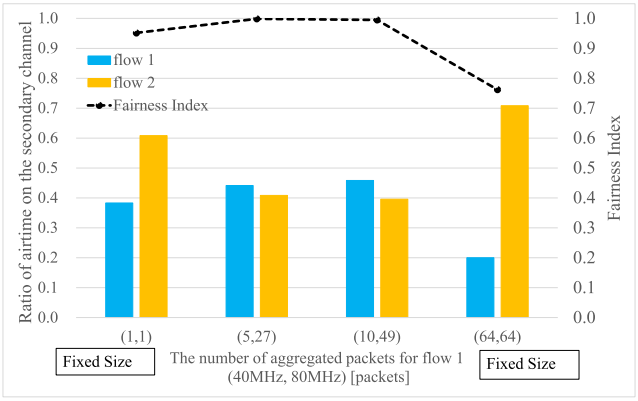

FIGURE 16. Ratio of airtime on the secondary channel for flows 1 and 2, and their fairness index.

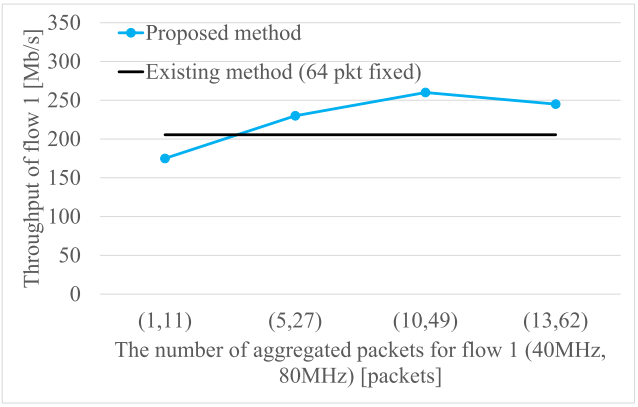

FIGURE 17. Throughput of flow 1.

requirement of flow 2 by equalizing the use of each flow time of the contention channel in flow 1 (maximum bonding width) and flow 2, the utilization time of the contention channel for each flow was used as an evaluation index. Furthermore, it is necessary for the contention throughput of flow 2 to maintain 50% of the single-unit throughput performance. Thus, we used the throughput of each flow and the ratio of the airtime in the secondary channel in the simulation to evaluate the performance.

B. SIMULATION RESULTS

First, we determine the optimal A-MPDU size for the environment, as shown in Fig. 13. Fig.15 shows the optimal number of aggregated packets determined from (18) when $X = 80$ and $Y = 40$. Furthermore, the ratio of the sum of airtime on the secondary channel for flows 1 (in the case of 80 MHz) and flow 2 to the simulation time (12 s) is shown in Fig. 16. Furthermore, Jain's fairness index [32] of the ratio of the sum of airtime of flows 1 and 2 on the secondary channel is shown in Fig. 16. Jain's fairness index can be derived from:

$$F_i = \frac{\left(\sum_{i=0}^{n} AT_i\right)^2}{n \sum_{i=0}^{n} AT_i^2}, \tag{19}$$

where AT_i indicates the ratio of the sum of the airtime of flow i, n is the number of flows. Then, all AT_i values are the same if F_i equals 1. In Fig. 16, $x1$ on the x-axis indicates the A-MPDU size of flow 1 in the case of contention with flow 2, and $x2$ is the maximum A-MPDU size of flow 1. In the case of (5, 27) and (10, 49), the difference between the ratio of the utilization time of the 80-MHz-width channel for flow 1 and that of the channel for flow 2 is smaller than that of the existing fixed-size A-MPDU method (the case of (1, 1) and (64, 64)). We can see that flows 1 and 2 can use the contention channel evenly in the case of (5, 27) and (10, 49), and then the Fairness index almost equals 1. Therefore, our proposed A-MPDU adaptation method achieves airtime fairness between two contended flows at the secondary channel.

Suppose the AP employs SCB; it cannot transmit any data until it obtains access to the entire channel for the SCB, including the competitive channel. The airtime of the AP with the SCB was the only airtime of flow 1 in the secondary channel (Fig. 16). Hence, the throughput of the AP with SCB decreases because it cannot use the airtime of flow 2. However, if the AP employs a DCB, it can send data within the shrunken channel during the airtime of flow 2. Therefore, DCB with A-MPDU adaptation is more effective in improving resource utilization in a channel-competitive environment.

Figs. 17 and 18 show the simulation results for the throughput performances of flows 1 and 2, respectively. Furthermore, Fig. 19 shows the total throughput of flow1 and flow2. The x-axis in Figs. 17, 18, and 19 represents

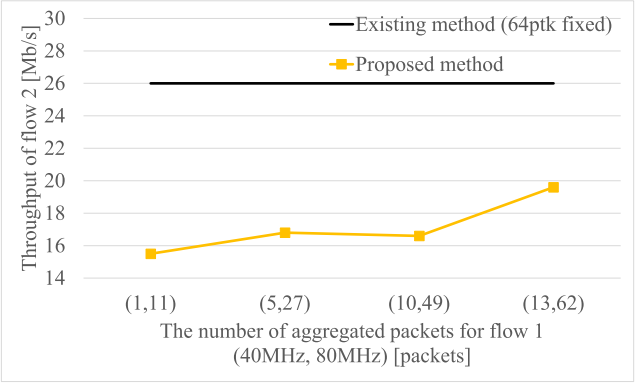

FIGURE 18. Throughput of flow 2.

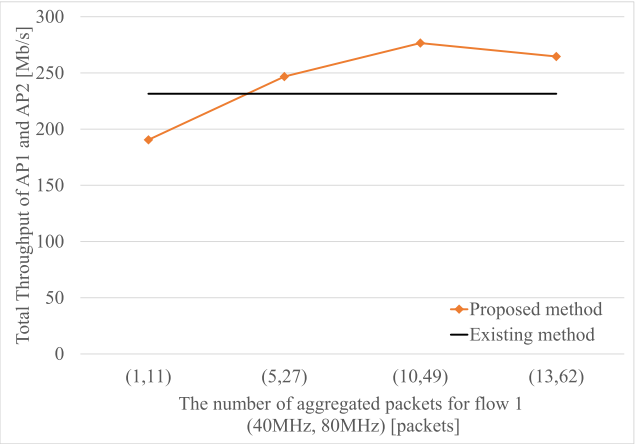

FIGURE 19. Total Throughput of flow 1 and 2.

$(x1, x2)$, where $x1$ is the A-MPDU size of flow 1 in the case of contention with flow 2, and $x2$ is the maximum A-MPDU size of flow 1. "Existing method" in the figure indicates the throughput for a fixed A-MPDU size (64 packets). For the proposed method, we focused on the throughput of flow 1. The throughput increased as the A-MPDU size of flow 1 increased. This is because, as the A-MPDU frame size increases, the amount of data to be transmitted increases, and the overhead (e.g., frame header, DIFS, and back-off of the CSMA/CA function) decreases. In contrast, the throughput of flow 2 obtained using the proposed method is smaller than that obtained using the existing fixed A-MPDU method because of the decreased competition in obtaining channel access. However, because 50% of the throughput without contention is 16.87 Mb/s, the requirement for flow 2 is almost satisfied when the number of aggregated packets is set to $(5, 27)$, $(10, 49)$, and $(13, 62)$. Alternatively, the throughput of flow 1 for DCB communication increases by more than 20 Mb/s when the number of aggregated packets for flow 1 is $(5, 27)$, $(10, 49)$, and $(13, 62)$. For the total throughput of flows 1 and 2 in Fig. 19, our proposed method achieved a maximum at the $(10, 49)$, and we found the optimal number of aggregate packets for air-time fairness in the WLAN with DCB.

These results show that in the environment shown in Fig. 13, the requirements for flows 1 and 2 can be satisfied simultaneously, and (18) is applicable to 80–40-MHz DCB. We also confirm that the proposed method is also effective in 40–20-MHz and in 80-20-MHz DCB environments, however we are afraid that the details of the simulation results of 40-20MHz and 80-20-MHz are not shown for lack of the space.

VII. DISCUSSION

Our evaluation environment was an ideal wireless environment with a high SINR and no interference; therefore, we assumed that there was no frame retransmission. Furthermore, we assumed that the required bandwidth of the application was heavy; therefore, the traffic load was heavy for the two competitive WLANs. Thus, the simulation results indicated the maximum effectiveness of the proposed method. Hence, we have discussed the revised points required for the proposed method.

First, the frame retransmission must be addressed. Frame retransmission occurs frequently in low-SINR environments. The number of aggregated frames and the DCB bandwidth should be determined based on the retransmission frame size and number of retransmission frames. However, the communication procedure implementation for frame retransmission differs between commercially available APs and STAs [33], [34]. Therefore, we calculated the number of aggregated frames for retransmission based on various frame retransmission procedures.

Second, we need to consider the power consumption of wireless devices. Internet of Things (IoT) devices are widely available and connected to the Internet. Many of these are small devices driven by batteries. Therefore, the power consumption of battery-driven wireless devices should be considered. A DCB can increase the power consumption of APs and STAs depending on the channel bandwidth; for example, the power consumption doubles if two channels are bonded. Thus, the application of CB is not recommended for WLANs from the perspective of power consumption. Furthermore, FA can increase the power consumption of APs and STAs, depending on the frame transmission duration. APs are always connected to wall sockets; hence, there is no power consumption issue. Meanwhile, battery-driven STAs have power consumption issues that should be addressed, particularly when considering the power consumption of STAs in WLAN with DCB and FA. The proposed method should also be adapted to the power consumption of battery-driven STAs. We expect resource unit (RU) allocation in IEEE802.11ax WLANs to be useful for addressing the power consumption issues of battery-driven STAs because each RU has a lower bandwidth than the entire channel bandwidth with CB. Therefore, the proposed method can be adapted to IEEE802.11ax OFDMA.

VIII. CONCLUDING REMARKS

In this study, we investigated the DCB performance based on the frame level with CSMA/CA. We introduced the $2\times$M/M/1/K queueing theory and implemented the DCB

mechanism in Scenargie. We validated the effectiveness of the simulations by comparing the obtained results with analytical results. The DCB performance significantly decreases in an environment in which a WLAN employing DCB competes with another WLAN, resulting in partially overlapping channels. This is attributed to the PA problem. Therefore, we propose a dynamic A-MPDU-size adaptation method to achieve airtime fairness. Simulation results show that the proposed scheme can improve throughput performance because of the dynamic A-MPDU-size adaptation while ensuring 50% throughput performance for competitive communication. These results demonstrate that dynamic A-MPDU-size adaptation, according to the DCB channel width is essential for achieving fair resource utilization in DCB-based WLAN environments.

In future studies, we will develop a dynamic A-MPDU-size adaptation method based on the RU tones in the OFDMA employed in the IEEE 802.11ax standard.

ACKNOWLEDGMENT

The authors would like to thank Yusuke Shimizu, for implementing the DCB function in Scenargie 2.2.

REFERENCES

[1] ERICCSON. (Jun. 2023). *Mobility Report Data and Forecasts, Mobile Data Traffic Outlook*. [Online]. Available: https://www.ericsson.com/en/reports-and-papers/mobility-report/dataforecasts/mobile-traffic-forecast

[2] *IEEE 802.11TM Wireless Local Area Networks, The Working Group for WLAN Standards*. Accessed: Jun. 1, 2023. [Online]. Available: http://www.ieee802.org/11//

[3] *IEEE Standards Association, IEEE Std 802.11ac-2013*. Accessed: Jun. 1, 2023. [Online]. Available: http://www.ieee802.org/11/

[4] S. Byeon, C. Yang, O. Lee, K. Yoon, and S. Choi, "Enhancement of wide bandwidth operation in IEEE 802.11ac networks," in *Proc. IEEE Int. Conf. Commun. (ICC)*, Jun. 2015, pp. 1547–1552.

[5] M. Heusse, F. Rousseau, G. Berger-Sabbatel, and A. Duda, "Performance anomaly of 802.11b," in *Proc. 22nd Annu. Joint Conf. IEEE Comput. Commun. Societies*, vol. 2, Mar. 2003, pp. 836–843.

[6] *Scenargie*. Accessed: Jun. 1, 2023. [Online]. Available: https://www.spacetime-eng.com/jp/products?page=Products_Scenargie_Visual_Lab_Base_Simulator_jp

[7] Y. Shimizu, D. Nobayashi, H. Tamura, and K. Tsukamoto, "Dynamic A-MPDU adaptation method for airtime fairness in channel bonding-ready WLANs," in *Proc. IEEE Pacific Rim Conf. Commun., Comput. Signal Process. (PACRIM)*, Aug. 2019, pp. 1–6.

[8] D. Skordoulis, Q. Ni, H.-H. Chen, A. P. Stephens, C. Liu, and A. Jamalipour, "IEEE 802.11n MAC frame aggregation mechanisms for next-generation high-throughput WLANs," *IEEE Wireless Commun.*, vol. 15, no. 1, pp. 40–47, Feb. 2008.

[9] J. Liu, M. Yao, and Z. Qiu, "Enhanced two-level frame aggregation with optimized aggregation level for IEEE 802.11n WLANs," *IEEE Commun. Lett.*, vol. 19, no. 12, pp. 2254–2257, Dec. 2015.

[10] A. C. Akpanobong, M. Othman, and G. O. Ansa, "Extending throughput performance for low SNR scenarios in WLANs using two-level frames aggregation with enhanced A-MSDU," *Wireless Pers. Commun.*, vol. 115, no. 2, pp. 1695–1710, Nov. 2020.

[11] A. Chattopadhyay and A. Chandra, "IEEE 802.11ac vs 802.11ad for V2X: How many frames can we aggregate?" in *Proc. IEEE 33rd Annu. Int. Symp. Pers., Indoor Mobile Radio Commun. (PIMRC)*, Sep. 2022, pp. 913–918.

[12] B. S. Kim, H. Y. Hwang, and D. K. Sung, "Effect of frame aggregation on the throughput performance of IEEE 802.11n," in *Proc. IEEE Wireless Commun. Netw. Conf.*, Mar. 2008, pp. 1740–1744.

[13] B. Ginzburg and A. Kesselman, "Performance analysis of A-MPDU and A-MSDU aggregation in IEEE 802.11n," in *Proc. IEEE Sarnoff Symp.*, Apr. 2007, pp. 1–5.

[14] Y. Lin and V. W. S. Wong, "WSN01-1: Frame aggregation and optimal frame size adaptation for IEEE 802.11n WLANs," in *Proc. IEEE Globecom*, Nov. 2006, pp. 1–6.

[15] M. Alaslani, A. Showail, and B. Shihada, "Green frame aggregation scheme for Wi-Fi networks," in *Proc. IEEE 16th Int. Conf. High Perform. Switching Routing (HPSR)*, Jul. 2015, pp. 1–6.

[16] X. He, F. Y. Li, and J. Lin, "Link adaptation with combined optimal frame size and rate selection in error-prone 802.11n networks," in *Proc. IEEE Int. Symp. Wireless Commun. Syst.*, Oct. 2008, pp. 733–737.

[17] M. Kim, E.-C. Park, and C.-H. Choi, "Adaptive two-level frame aggregation for fairness and efficiency in IEEE 802.11n wireless LANs," *Mobile Inf. Syst.*, vol. 2015, pp. 1–14, Jan. 2015.

[18] W. H. Lee and H. Y. Hwang, "A-MPDU aggregation with optimal number of MPDUs for delay requirements in IEEE 802.11ac," *PLoS ONE*, vol. 14, no. 3, Mar. 2019, Art. no. e0213888, doi: 10.1371/journal.pone.0213888.

[19] S. Seytnazarov and Y.-T. Kim, "QoS-aware adaptive A-MPDU aggregation scheduler for voice traffic in aggregation-enabled high throughput WLANs," *IEEE Trans. Mobile Comput.*, vol. 16, no. 10, pp. 2862–2875, Oct. 2017.

[20] T. Høiland-Jørgensen, M. Kazior, D. Täht, and P. Hurtig, "Ending the anomaly: Achieving low latency and airtime fairness in Wi-Fi," in *Proc. USENIX ATC*, 2017, pp. 139–151.

[21] S. Barrachina-Muñoz, F. Wilhelmi, and B. Bellalta, "Dynamic channel bonding in spatially distributed high-density WLANs," *IEEE Trans. Mobile Comput.*, vol. 19, no. 4, pp. 821–835, Apr. 2020.

[22] S. Chakraborty, S. K. Reddy K., R. Karmakar, and S. Chattopadhyay, "IEEE 802.11ac DBCA: A tug of war between channel utilization and fairness," in *Proc. IEEE Global Commun. Conf.*, Dec. 2017, pp. 1–6.

[23] M. Yazid and A. Ksentini, "Stochastic modeling of the static and dynamic multichannel access methods enabling 40/80/160 MHz channel bonding in the VHT WLANs," *IEEE Commun. Lett.*, vol. 23, no. 8, pp. 1437–1440, Aug. 2019.

[24] K. Kosek-Szott and N. Rapacz, "Tuning Wi-Fi traffic differentiation by combining frame aggregation with TXOP limits," *IEEE Commun. Lett.*, vol. 24, no. 3, pp. 700–703, Mar. 2020.

[25] V. A. Reddy, G. L. Stüber, S. Al-Dharrab, W. Mesbah, and A. H. Muqaibel, "Energy-efficient mm-wave backhauling via frame aggregation in wide area networks," *IEEE Trans. Wireless Commun.*, vol. 20, no. 10, pp. 6954–6970, Oct. 2021.

[26] G. Bianchi, "Performance analysis of the IEEE 802.11 distributed coordination function," *IEEE J. Sel. Areas Commun.*, vol. 18, no. 3, pp. 535–547, Mar. 2000.

[27] L. Simic, J. Riihijärvi, and P. Mähönen, "Measurement study of IEEE 802.11ac Wi-Fi performance in high density indoor deployments: Are wider channels always better?" in *Proc. IEEE 18th Int. Symp. World Wireless, Mobile Multimedia Netw. (WoWMoM)*, Jun. 2017, pp. 1–9.

[28] M. Han, S. Khairy, L. X. Cai, and Y. Cheng, "Performance analysis of opportunistic channel bonding in multi-channel WLANs," in *Proc. IEEE Global Commun. Conf. (GLOBECOM)*, Dec. 2016, pp. 1–6.

[29] T. Song, T.-Y. Kim, W. Kim, and S. Pack, "Channel bonding algorithm for densely deployed wireless LAN," in *Proc. Int. Conf. Inf. Netw. (ICOIN)*, Jan. 2016, pp. 395–397.

[30] C. Kai, Y. Liang, T. Huang, and X. Chen, "To bond or not to bond: An optimal channel allocation algorithm for flexible dynamic channel bonding in WLANs," in *Proc. IEEE 86th Veh. Technol. Conf. (VTC-Fall)*, Sep. 2017, pp. 1–6.

[31] H. Tamura, K. Kawahara, and Y. Oie, "Analysis of two-phase path management scheme for MPLS traffic engineering," *IEICE Trans. Commun.*, vols. E92–B, no. 1, pp. 59–67, 2009.

[32] D.-M. Chiu and R. Jain, "Analysis of the increase and decrease algorithms for congestion avoidance in computer networks," *Comput. Netw. ISDN Syst.*, vol. 17, no. 1, pp. 1–14, Jun. 1989.

[33] K. Fujii, H. Tamura, D. Nobayashi, and K. Tsukamoto, "Experimental investigation of static channel bonding performance in competitive environment—Impact of different MAC procedures in 802.11ac," in *Proc. 5th Int. Workshop Smart Wireless Commun. (SmartCom)*, 2018, vol. 118, no. 274, pp. 1–2.

[34] T. Oogami, H. Tamura, D. Nobayashi, and K. Tsukamoto, "Experimental evaluation of uplink communication performance in IEEE 802.11ax wireless local area network: OFDM vs. OFDMA," in *Advances in Intelligent Networking and Collaborative Systems* (Lecture Notes on Data Engineering and Communications Technologies). Cham, Switzerland: Springer, 2023, pp. 495–504.

HITOMI TAMURA (Member, IEEE) received the D.E. degree in computer sciences and electronics from Kyushu Institute of Technology (Kyutech), Japan, in 2005. From 2005 to 2007, she was a Postdoctoral Researcher with Kyutech. From 2007 to 2008, she was a Researcher with the Human Media Creation Center, Kyushu. From 2011 to 2021, she was an Assistant Professor with Fukuoka Institute of Technology. Since 2022, she has been an Associate Professor with Fukuoka Institute of Technology. She is a member of ACM, IPSJ, and IEICE.

DAIKI NOBAYASHI (Member, IEEE) received the B.E., M.E., and D.E. degrees from Kyutech, in 2006, 2008, and 2011, respectively. From April 2010 to March 2012, he was a Research Fellow with Japan Society for the Promotion of Science (JSPS). In 2012, he was an Assistant Professor with the Department of Electrical and Electronic Engineering, Faculty of Engineering, Kyutech. Since 2021, he has been an Associate Professor with the Department of Electrical and Electronic Engineering, Faculty of Engineering, Kyutech. He is a member of IEICE.

KENJI KAWAHARA (Member, IEEE) received the B.E. and M.E. degrees in computer sciences and electronics from Kyutech, in 1991 and 1993, respectively, and the Ph.D. degree in information and computer science from Osaka University, in 1996. From 1995 to 1997, he was an Assistant Professor with the Information Technology Center, Nara Institute of Science and Technology. From 1997 to 1999, he was an Assistant Professor and an Associate Professor with the Department of Computer Science and Electronics, Faculty of Computer Science and Systems Engineering, Kyutech, from 1999 to 2018. Since April 2018, he has been an Associate Professor with the Department of Computer Science and Networks, Kyutech. His research interests include computer networks, performance analysis based on the queueing theory in high-speed networks, and green ICT. He is a member of IEICE.

KAZUYA TSUKAMOTO (Member, IEEE) received the D.E. degree in computer science from Kyutech, in 2006. From April 2006 to March 2007, he was a JSPS Research Fellow with Kyutech. In 2007, he was an Assistant Professor with the Department of Computer Science and Electronics, Kyutech. He was an Associate Professor with the Department of Computer Science and Electronics, in 2013. He has been a Professor with the Department of Computer Science and Networks, since January 2022. His research interests include the performance evaluation of computer and wireless networks. He is a member of ACM, IPSJ, and IEICE.